

Document downloaded from:

<http://hdl.handle.net/10251/84338>

This paper must be cited as:

Shabir, Q.; Pokale, A.; Loni, A.; Johnson, DR.; Canham, L.; Fenollosa Esteve, R.; Tymczenko, MK.... (2011). Medically Biodegradable Hydrogenated Amorphous Silicon Microspheres. *Silicon*. 3(4):173-176. doi:10.1007/s12633-011-9097-4.



The final publication is available at

<http://doi.org/10.1007/s12633-011-9097-4>

Copyright Springer Verlag (Germany)

Additional Information

Medically Biodegradable Hydrogenated Amorphous Silicon Microspheres

A.Pokale, Q.Shabir*, A.Loni, D.R.Johnson and L.T.Canham

Intrinsic Materials Ltd, Malvern Hills Science Park, Geraldine Road, Malvern, Worcs
WR14 3SZ.

R. Fenollosa, M. Tymczenko, I. Rodríguez, and F.Meseguer

Centro de Tecnologías Físicas

Unidad Asociada ICMM-CSIC/UPV

CPI Edificio 8B Bloque K (cubo Gris)

Universidad Politécnica de Valencia

46022 Valencia, Spain

A.Cros and A. Cantarero

Instituto de Ciencia de Materiales

Universidad de Valencia

Poligono “La Coma” s/n 46980 Paterna, Valencia Spain

*Author for Correspondence: Qurrat Shabir currently at pSivida Ltd, Malvern, WR14
3SZ, UK.

email: <mailto:qshabir@psivida.com>.

Abstract

Hydrogenated amorphous silicon colloids of low surface area ($<5\text{m}^2/\text{g}$) are shown to exhibit complete in-vitro biodegradation into orthosilicic acid within 10-15 days at 37°C . When converted into polycrystalline silicon colloids, by high temperature annealing in an inert atmosphere, microparticle solubility is dramatically reduced. The data suggests that amorphous silicon does not require nanoscale porosification for full in-vivo biodegradability. This has significant implications for using a-Si:H coatings for medical implants in general, and orthopaedic implants in particular. The high sphericity and biodegradability

of submicron particles may also confer advantages with regards to contrast agents for medical imaging.

Key words

Silicon, amorphous, biodegradable, medical

Introduction

The biocompatibility of various nanostructures of the semiconductor silicon is receiving increasing attention for drug delivery, medical imaging and biosensing [1-3]. The in-vitro biodegradability of nanostructured porous forms of very high surface area was first revealed in the 1990's and its use for medical imaging purposes has been demonstrated in-vivo[4,5]. Mesoporous silicon is commonly derived by etching single crystal or polycrystalline wafers and powders and largely retains the crystallinity of such feedstocks [6]. Micromachined silicon, macroporous and large grain size polycrystalline silicon microparticles do not exhibit significant biodegradability, in-vitro nor in-vivo[7,8]. Chemical Vapor Deposition techniques (CVD) allow the formation of polydisperse silicon micro and nanoparticles, with size ranging from 0.5 to 5 micrometers, and with a highly spherical shape [9]. The combined low surface roughness, spherical topology and high refractive index, results in silicon "colloids" or microsphere assemblies working very well as optical microcavities in the IR region [10]. They can be porous, amorphous or polycrystalline, depending on the decomposition parameters [11]. Silicon colloids can be seen as a new enabling particulate system with many applications in materials science, photonics, cosmetics and sensing [9,10,12,13,14]. Here we report on the in-vitro biodegradability of nanostructured amorphous and polycrystalline silicon colloids. Our data shows much higher biodegradability of amorphous silicon colloids than that of nanostructured polycrystalline equivalents.

Experimental

Silicon colloids for biodegradability assays were fabricated by the method described elsewhere [9]. Amorphous silicon colloids were obtained by decomposing disilane at 450°C in a CVD reactor. Polycrystalline silicon colloids were achieved by annealing the amorphous colloids at 800°C for 1 hour in an argon inert atmosphere. Structural properties of the colloids were studied by using several techniques, namely Scanning Electron Microscopy (SEM), X Ray Powder Diffraction (XRD) and Raman Spectroscopy (RS). The samples for XRD analysis consist of big clusters, of 100 micrometers in height by 1 cm² in area approximately, containing many microspheres, which were deposited on silica substrates. We used an X-ray wavelength, $\lambda = 1.54187 \text{ \AA}$, and the spot size was about 4 mm diameter, therefore the obtained X-ray spectra correspond to an average signal produced by millions of microspheres. The samples for (RS) consist of isolated microspheres on silica substrates. Raman spectra were measured on single microspheres by using a Jobin-Ivon T64000 triple monochromator provided with a microprobe accessory and pumped with an Ar ion laser. The excitation wavelength was 545 nm, beam power of 10 μ W and spot size of 10 μ m, corresponding to a very low Micro-Raman excitation density of 10 Wcm⁻². There were thus small beam heating effects, as it is well known that

temperature rises can significantly affect Raman lineshape and position [6].

Gas adsorption/desorption analysis was carried out on a Micromeritics Tristar instrument with sample de-gassing at 70°C under vacuum for 1hr and BET analysis of the isotherms.

In-vitro biodegradability into orthosilicic acid was quantitatively assessed using a molybdenum blue based assay [15]. Sealed plastic containers of 200ml volume containing 5mg silicon samples in trizma buffer (pH 7.4 at 37C) were agitated at 50rpm in a water bath for periods up to 10 days. Aliquots of 2.5ml were withdrawn for analysis at predetermined time points. These were acidified, reacted with 1% disodium EDTA, then 5% ammonium molybdate and then 17% sodium sulphite solution. Their resulting absorbance at 700nm was then converted to an orthosilicic acid concentration by comparison with standard solutions of known concentration.

Results

Figure 1 shows the highly spherical nature of the microparticles. The colloids have a diameter from 0.5 to 5 micrometers, and the mean diameter is 1.8 micrometers. The density of a-Si:H is a strong function of the hydrogen content and other factors. Assuming a value of 1.9g/cm³ (equivalent to about 20 atomic % H) and perfectly spherical particles (surface area of $4\pi r^2$), gives a theoretical value of 1.7m²/g for the surface area of a non-porous colloid [16]. BET analysis gave a value of 1.8m²/g, which is in good agreement. This demonstrates that the amorphous microparticle colloid possesses minimal microporosity and mesoporosity. Indeed optical scattering from single particles is sensitive to both chemical composition and porosity with hollow particles having completely different scattering spectra to those of the compact particles under study here [9].

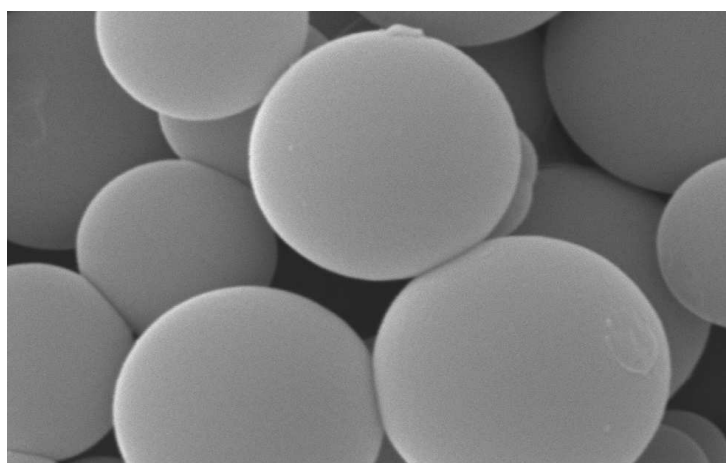


Figure 1. SEM image of silicon colloids obtained by a hot wall CVD process where disilane was decomposed at 450 ° C.

Figure 2 shows XRD normalized spectra of amorphous (a) and polycrystalline (b) silicon colloids. Trace (c) corresponds to a reference sample made of single crystal silicon powder. The amorphous nature of the colloids, that were grown at 450°C, can be deduced from the wide feature of trace (a). Trace (b) confirms that the annealing process, at 800 °C, transforms the amorphous silicon phase into the polycrystalline one.

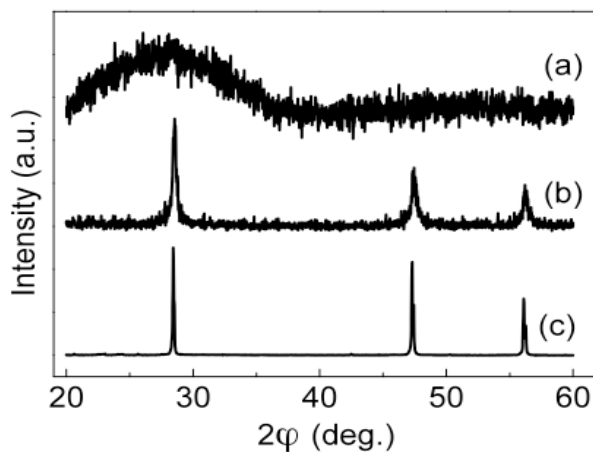


Figure 2. XRD spectra of (a) amorphous and (b) polycrystalline silicon colloids, (c) corresponds to single crystal silicon sample powder.

The application of the Scherrer equation to the peak centered around $2\phi=28^\circ$ gives a crystallite size of about 30 nm [17]. This transformation can also be seen through micro-Raman analysis, as it is illustrated by the spectra (a), (b) and (c) of Figure 3, that correspond to amorphous, polycrystalline and the reference sample respectively. These spectra have been normalized and they were measured on single microspheres.

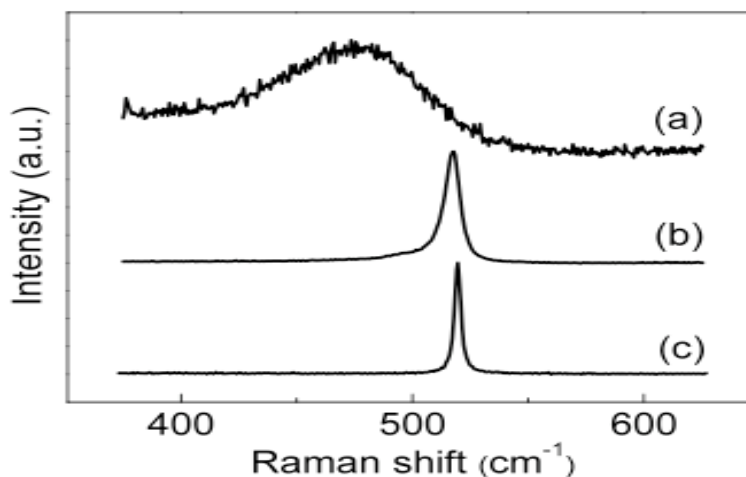


Figure 3. Raman spectra of single amorphous (a) and polycrystalline (b) silicon colloids. (c) Corresponds to a reference spectrum of single crystal silicon.

The broadening and the red shift of the Raman peak of trace (b), compared to the reference crystalline silicon sample (c), is in good agreement with the small crystallite size of the polycrystalline colloid and confirms the characterization performed by X-ray measurements.

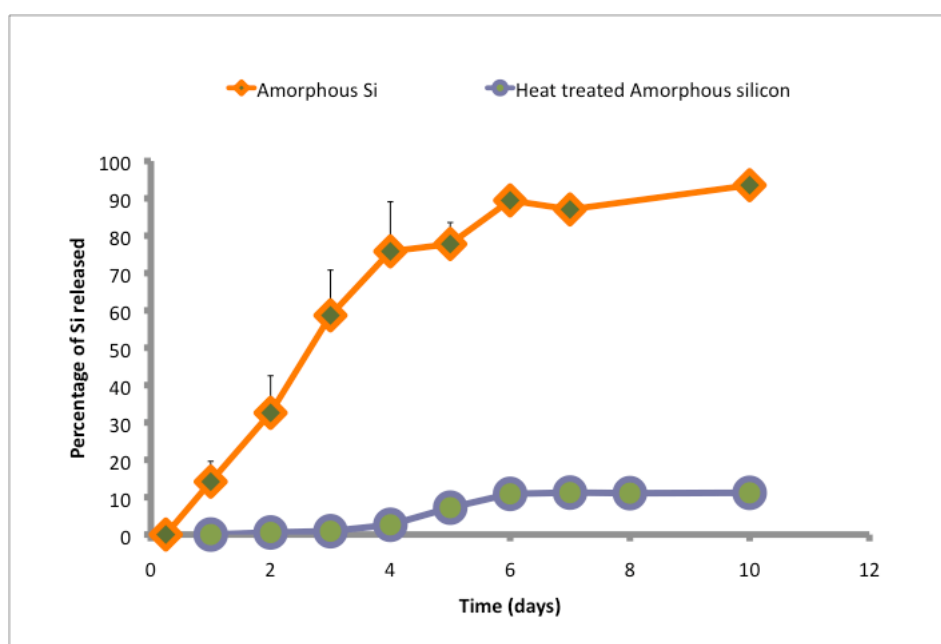


Figure 4. Dissolution of heat-treated and untreated amorphous silicon particles in pH 7.0 buffered media.

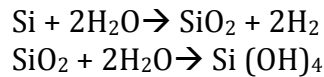
Figure 4 compares the solubility of hydrogenated amorphous silicon with thermally crystallized material of similar particle size distribution. Whereas the amorphous colloid undergoes >90% dissolution within 10 days, the equivalent polycrystalline colloid (microspheres with 30nm grain size) has lost under 10% of its mass and maintains a stable weight after the first few days.

Discussion & conclusions

We believe this is the first time that the biodegradability of amorphous semiconducting silicon has been quantitatively assessed. Biodegradation of silicon nanostructures has been monitored ex-situ by electron microscopy of the material remaining or by a chemical method measuring the accumulation of biodegradable products (18,1,2). In this study we opted for the latter technique to provide quantification data on degradation kinetics of silicon structures.

Porous silicon in aqueous conditions undergoes hydrolysis to form orthosilicic acid and the reaction is catalyzed by OH⁻, hence the rate of dissolution increases with increasing pH.

Dissolution of unoxidised silicon can be described with a simplified two step process.



The oxidative first step generates hydrogen gas and is dependent on both electronic band gap and doping of the semiconductor. Complete hydrolysis of the oxide phase then generates orthosilicic acid, which is the natural bioavailable form of silicon, freely diffusible in human tissues, and readily excreted via the kidneys [4,19].

The biodegradation study is carried out at pH 7.4 and 37°C conditions to mimic *in vivo* conditions.

During a study of the bioactivity of deposited nanocrystalline silicon layers it was noted that layers which were virtually amorphous underwent significant corrosion in simulated human plasma, but the etch rate was not quantified [18]. Here we have directly compared the in-vitro solubility of amorphous and polycrystalline powder of the same particle size distribution.

It is interesting to compare this result with that of silica where the equilibrium solubility of the amorphous phase in water is approximately 10 times higher than that of crystalline quartz [19]. Quartz is very resistant to hydrolysis and does not biodegrade in physiological environments. Certain forms of high surface area, amorphous mesoporous silica however does show biodegradability whilst others show high stability against hydrolysis [20, 21]. It seems likely that amorphous silicon in various structural forms will show much faster biodegradation kinetics to those of both amorphous silica and polycrystalline silicon. This has encouraging implications for the use of amorphous silicon coatings in medical implant applications where a temporary structure conveys advantages in device efficacy and biocompatibility regarding its intended use. The observation of its full biodegradability without porosification will expand the fabrication options in this regard. Mesoporosity is a major attribute for applications such as drug delivery but there are numerous uses in orthopedics and orthopedic tissue engineering where controlled silicic acid release is used to stimulate bone growth [1,2,22]. Fully biodegradable spheres of submicron diameter are also of interest as contrast agents for both in-vitro and in-vivo medical imaging [23]. The biocompatibility of hydrogenated amorphous silicon is worthy of detailed assessment.

Acknowledgements

This work has been partially supported by the Spanish CICYT projects, FIS2009-07812, Consolider CSD2007-046, MAT2009-010350 and PROMETEO/2010/043.

References

- [1] Salonen J, Kaukonen AM, Hirvonen J, Lehto VP (2008) *J Pharmaceutics* 97:632-653
- [2] Anglin E, Cheng L, Freeman WR, Sailor MJ (2008) *Adv Drug Delivery Reviews* 60:1266-1277
- [3] O'Farrell N, Houlton A, Horrocks BR (2006) *Int J Nanomedicine* 1:451-472
- [4] Canham LT, *Adv Mater*, 1995, 7,1037; PCT patent WO 97/06101,1999.
- [5] Park JH, Gui L, Malzahn G, Ruoslahti E, Bhatia SN, Sailor MJ (2009) *Nature Mater* 8:331 -336
- [6] Cullis AG, Canham LT, Calcott PDJ (1997) *J Appl Phys* 82:909-966
- [7] Canham LT, Reeves CR (1996) *Mat Res Soc Symp* 414:189-190
- [8] Edell DJ, Toi VV, McNeil VM, Clark LD (1992) *IEEE Trans Biomed Eng*, 39:635-643
- [9]{a} Fenollosa R, Meseguer F, Tymczenko M (2008) *Adv Mater* 20:95
- {b} Fenollosa R, Meseguer F, Tymczenko M, Spanish Patent P200701681, 2007
- {c} Pell LE, Schricker AD, Mikulec FV, Korgel BA (2004) *Langmuir* 20:6546.
- [10] Xifré-Perez E, Fenollosa R, and Meseguer F (2011) *Opt Express* 19: 3455-3463
- [11] Fenollosa R, Ramiro-Manzano F, Tymczenko M, Meseguer F (2010) *J Mater Chem* 20: 5210.
- [12] Xifré-Pérez E, Domenech JD, Fenollosa R, Muñoz P, Capmany J, Meseguer F (2011) *Opt Express* 19-4: 3185-3192
- [13] Rodriguez I, Fenollosa R, Meseguer F (2010) *Cosmetics & Toiletries* 42-49
- [14] Ramiro-Manzano F, Fenollosa R, Meseguer F, Xifré-Pérez E, Garin M (2011) *rymhn . Adv Material*. Doi:10.1002/adma.201100986.
- [15] Iler RK (1979) In: *Chemistry of Silica: Solubility, polymerization, colloid & surface properties & Biochemistry*, John Wiley & Sons, New York.
- (16) Tanaka K, Maruyama E, Shimado T, Okamoto H (1999) *Amorphous Silicon*, John Wiley & Sons, New York
- [17] Patterson AL (1939) *Phys Rev* 56: 978-982
- [18] Canham LT, Reeves CL, King DO, Branfield PJ, Gabb JG, Ward MC (1996) *Adv Mater* 8: 850-852
- [19] Iler RK In: *Chemistry of Silica: Solubility, polymerization, colloid & surface properties & Biochemistry*, John Wiley & Sons, New York.

[20] Finnie KS, Waller DJ, Perret FL, Krause-Heuer AM, Lin HQ, Hanna JV, Barbe CJ (2009) J Sol-Gel Technol 49 :12-18

[21] Zhao D, Huo Q, Feng J, Chmelka BF, Stucky GD (1998) J Am Chem Soc 120:6024-6036

[22] Fan D, Akkaraju GR, Couch EF, Canham LT, Coffey JL (2010) Nanoscale, 1:354-361

[23] Tasciotti E, Godin B, Martinez JO, Chiappini C, Bhavane R, Liu X, Ferrari M (2011) Mol Imaging 10:56-58

